PROCEEDINGS OF SCIENCE

The QCD static energy at short distances

Joan Soto
Departament d'Estructura i Constituents de la Matèria and Institut de Ciències del Cosmos, Universitat de Barcelona, Diagonal 647, 08028 Barcelona, Catalonia, Spain
E-mail: joan.soto@ub.edu

I review the status of the calculations of the QCD static energy at short distances, including renormalization group and renormalon analysis. Applications to heavy quarkonium physics are briefly discussed.

8th Conference Quark Confinement and the Hadron Spectrum
September 1-6 2008
Mainz, Germany

PoS(Confinement8)004

1. The QCD static energy

The QCD static energy ($E(r)$), namely the ground state energy of a static quark and a static antiquark separated at a distance r, is a basic object to understand the dynamics of QCD [1]. Nowadays, there exist very precise calculations in lattice QCD in the case of pure gluodynamics ($N_f = 0$) [2]. At long distances, it increases linearly in r, a sign of confinement, and its behavior is well reproduced by an effective string theory [3]. At short distances, one may naïvely expect $E(r) = \alpha_E(r)/r$, with $\alpha_E(r)$ computable in perturbation theory in α_s, i.e. $\alpha_E(r) = \sum_{n=0}^{\infty} a_n \alpha_s^{n+1}(1/r)$. However, a_3 turns out to be IR divergent and resummations are required to obtain a finite result [4], as it will be discussed in the next section. In fact, a detailed renormalization group and renormalon analysis is necessary for the perturbative calculations to match lattice results.

The QCD static energy is closely related to the potentials to be input in the Schrödinger equation which describes heavy quarkonium systems, like charmonium, bottomonium, B_c and would-be-toponium. Its short distance behavior is relevant for the ground states of these systems, specially for the latter.

2. The QCD static energy at short distances

As mentioned above, a calculation of $E(r)$ in perturbation theory (PT) of α_s fails starting at three loops. The reason is that a static quark and a static antiquark can not only be in a singlet configuration but also in an octet one. At lower order $E(r)$ coincides with the energy of the singlet configuration, $E(r) \simeq E_s(r) \sim -C_F \alpha_s/r < 0$. The energy of the octet configuration is positive, $E_o(r) \sim -(C_F - C_A/2)\alpha_s/r > 0$, and hence larger. However, at higher orders virtual singlet to octet transitions mediated by gluons of energy $\sim \alpha_s/r$ may occur. For these gluons, α_s/r is not a small quantity, and hence PT cannot be used [4].

We can clearly identify two relevant energy scales in the problem, $1/r$, the soft scale, and α_s/r, the ultrasoft scale. For $r \to 0$ they are well separated, and hence effective field theories (EFT) are expected to be useful in higher order calculations.

3. Potential Non-Relativistic QCD

The EFT which is suitable for higher order calculations of $E(r)$ at short distances is Potential Non-Relativistic QCD (pNRQCD) in the weak coupling regime [5, 6] (see [7] for a review). It is obtained from the static limit of QCD, or equivalently from Heavy Quark Effective Theory for a quark and an antiquark, by integrating out in PT gluons of energy $\sim 1/r$, and leaving as explicit degrees of freedom those of energy $\sim \alpha_s/r$. Its Lagrangian reads,

$$\begin{aligned}\mathscr{L}_{\rm pNRQCD} = & \int d^3\mathbf{r}\, {\rm Tr}\left\{ {\rm S}^\dagger \left(i\partial_0 - V_s(\mathbf{r},\mu)\right) {\rm S} + {\rm O}^\dagger \left(iD_0 - V_o(\mathbf{r},\mu)\right) {\rm O} \right\} \\ & + V_A(r,\mu) {\rm Tr}\left\{ {\rm O}^\dagger \mathbf{r}\cdot g\mathbf{E}\, {\rm S} + {\rm S}^\dagger \mathbf{r}\cdot g\mathbf{E}\, {\rm O} \right\} + \\ & + \frac{V_B(r,\mu)}{2} {\rm Tr}\left\{ {\rm O}^\dagger \mathbf{r}\cdot g\mathbf{E}\, {\rm O} + {\rm O}^\dagger {\rm O}\mathbf{r}\cdot g\mathbf{E} \right\} + \cdots\end{aligned}$$

V_s, V_o,V_A, V_B, are matching coefficients calculable in PT in $\alpha_{\rm s}(1/r)$. V_s and V_o are the singlet and octet potentials respectively. The status of the calculations is the following. For the singlet potential we have,

$$\begin{aligned} V_s(r,\mu) \,=\, & -\frac{C_F\alpha_{\rm s}(1/r)}{r}\Bigg\{1+\frac{\alpha_{\rm s}(1/r)}{4\pi}\,[a_1]+\left(\frac{\alpha_{\rm s}(1/r)}{4\pi}\right)^2[\tilde{a}_2] \\ & +\left(\frac{\alpha_{\rm s}(1/r)}{4\pi}\right)^3\left[a_3^L\log\mu r+\tilde{a}_3\right] \\ & +\left(\frac{\alpha_{\rm s}(1/r)}{4\pi}\right)^4\left[a_4^{L2}\log^2\mu r+a_4^L\log\mu r+\tilde{a}_4\right]+\cdots\Bigg\}, \end{aligned}$$

The one-loop coefficient a_1 was calculated in [8], the two loop singlet coefficient a_2 in [9]. The logarithmic piece of the third-order correction a_3^L was calculated in [10], whereas the non-logarithmic piece $\tilde{a}_3$ has not been completely calculated yet. The fermionic contributions of $\tilde{a}_3$ has very recently been presented in [11], and the computation of the N_f independent piece is reported to be in progress. A Padé estimate of $\tilde{a}_3$ may be found in [12]. The double logarithmic coefficient a_4^{L2} may be obtained from [13] and the logarithmic coefficient a_4^L was obtained in [14]. $\tilde{a}_4$ remains unknown. For the octet potential we have,

$$\begin{aligned} V_o(r,\mu) \,=\, & -\frac{(C_F-C_A/2)\alpha_{\rm s}(1/r)}{r}\Bigg\{1+\frac{\alpha_{\rm s}(1/r)}{4\pi}\,[b_1] \\ & +\left(\frac{\alpha_{\rm s}(1/r)}{4\pi}\right)^2[\tilde{b}_2]+\left(\frac{\alpha_{\rm s}(1/r)}{4\pi}\right)^3\left[b_3^L\log\mu r+\tilde{b}_3\right] \\ & +\left(\frac{\alpha_{\rm s}(1/r)}{4\pi}\right)^4\left[b_4^{L2}\log^2\mu r+b_4^L\log\mu r+\tilde{b}_4\right]+\cdots\Bigg\}, \end{aligned}$$

The one-loop coefficient $b_1=a_1$. The two loop octet coefficient b_2 was calculated in [15]. The logarithmic piece of the third-order correction b_3^L was calculated in [6]. The double logarithmic coefficient b_4^{L2} may be obtained from [13] and the logarithmic coefficient b_4^L has been obtained in [16]. $\tilde{b}_3$ and $\tilde{b}_4$ remain unknown. For the singlet-octet and octet-octet transition potentials we have,

$$\begin{aligned} V_i(r,\mu) \,=\, & 1+\left(\frac{\alpha_{\rm s}(1/r)}{4\pi}\right)\left[c_{i1}^L\log\mu r+\tilde{c}_{i1}\right] \\ & +\left(\frac{\alpha_{\rm s}(1/r)}{4\pi}\right)^2\left[c_{i2}^{L2}\log^2\mu r+c_{i2}^L\log\mu r+\tilde{c}_{i2}\right]+\cdots \end{aligned}$$

$i=A,B$. c_{i1}^L and c_{i2}^{L2} where found to vanish in [13]. $\tilde{c}_{i1}$ and c_{i2}^L, have also been found to vanish in [16]. $\tilde{c}_{i2}$ remain unknown.

The calculation of $E(r)$ in pNRQCD is thus divided in two steps: (i) the calculation of the potentials, namely the matching coefficients above, and (ii) the calculation of ultrasoft loops. The latter at NNNLO corresponds to the right most diagram in fig. 1. The outcome of the calculation reads,

$$E(r) \,=\, V_s(r,\mu)+[\text{US loop}](V_s,V_o,V_A,\mu)$$

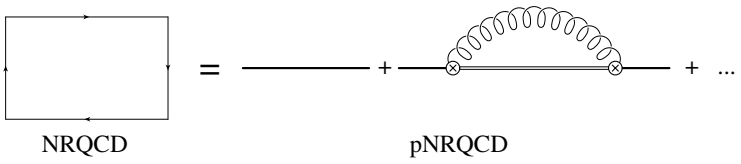

Figure 1: The single and double lines correspond to the singlet and octet propagators respectively.

$$= -\frac{C_F\alpha_{\rm s}(1/r)}{r}\left\{1+\frac{\alpha_{\rm s}(1/r)}{4\pi}[a_1]+\left(\frac{\alpha_{\rm s}(1/r)}{4\pi}\right)^2[\tilde{a}_2]\right.$$
$$\left.+\left(\frac{\alpha_{\rm s}(1/r)}{4\pi}\right)^3\left[a_3^L\log\frac{C_A\alpha_{\rm s}(1/r)}{2}+\tilde{a}_3\right]+\cdots\right\}$$

Note the cancellation of the factorization scale dependence μ between the potentials and the ultrasoft contributions.

4. Renormalization Group

Since physical observables cannot depend on the factorization scale, the potentials above obey renormalization group equations, which at NNLL read [13],

$$\begin{cases}\mu\dfrac{d}{d\mu}V_s=\gamma_s(\alpha_{\rm s})V_A^2\,(V_o-V_s)^3\,r^2\\ \mu\dfrac{d}{d\mu}V_o=\gamma_o(\alpha_{\rm s})V_A^2\,(V_o-V_s)^3\,r^2\\ \mu\dfrac{d}{d\mu}V_A=\gamma_A(\alpha_{\rm s})V_A\\ \mu\dfrac{d}{d\mu}V_B=\gamma_B(\alpha_{\rm s})V_B\end{cases},$$

where the anomalous dimensions $\gamma_i(\alpha_{\rm s})$, $i=s,o,A,B$ are needed at order $\alpha_{\rm s}(\mu)$..

$$\gamma_s(\alpha_{\rm s})=-\frac{2}{3}\frac{\alpha_{\rm s}C_F}{\pi}\quad,\quad\gamma_o(\alpha_{\rm s})=-\frac{\gamma_s(\alpha_{\rm s})}{N_c^2-1}\quad,\quad\gamma_A(\alpha_{\rm s})=\gamma_B(\alpha_{\rm s})=0$$

By solving the RG equations, the static energy at NNLL can be obtained [13],

$$E(r)\,=\,V_s(r,\mu)=V_s(r,1/r)+\,2\frac{N_c^2-1}{N_c^2}\left[(V_o-V_s)(1/r)\right]^3r^2\frac{\gamma_{os}^{(0)}}{\beta_0}\ln\frac{\alpha_{\rm s}(\mu)}{\alpha_{\rm s}(1/r)}$$

$\gamma_{os}^{(0)}=N_c/3,\quad\mu\sim C_A\alpha_{\rm s}(1/r)/2r$

5. Renormalons

An important problem concerning the practical usefulness of the results above is the fact that $V_s(r,\mu)$ does not converge well when it is calculated in the $\overline{\rm MS}$ scheme, as illustrated in fig. 2. This bad behavior may be interpreted as: (i) emanating from a renormalon singularity close to the origin

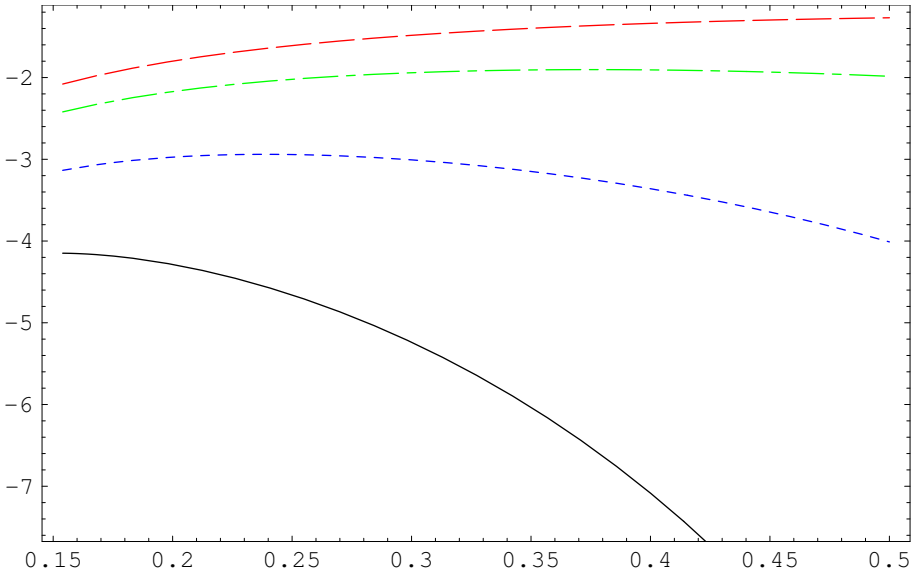

Figure 2: Plot of $r_0 V_s(r,\mu)$ (y-axis) versus r/r_0 (x-axis) at tree (dashed line), one-loop (dash-dotted line), two-loops (dotted line) and three loops (estimate [12]) plus the RG expression for the ultrasoft logs (solid line). $\mu = 2.5\, r_0^{-1}$, $r_0^{-1} \sim 400 MeV$. Plot taken from ref. [17].

in the positive real axes of the Borel plane, or (ii) signaling that non-perturbative contributions are important. If both interpretations are correct, one may devise a strategy to bring the calculation back into control: (i) find the operators which may account for the non-perturbative effects, (ii) impose that the ambiguities in the definition of the Borel transform are accounted for these operators, (iii) reshuffle suitable contributions in the perturbative series related to the renormalon singularity into the operators.

In our case the lower dimensional operators are those related to the residual mass term in HQET which are inherited in pNRQCD. They can be accounted for by making the shift $V_{s,o}(r,\mu) \to V_{s,o}(r,\mu) + \Lambda_{s,o}(r,\mu)$, $\Lambda_{s,o}(r,\mu) = \mathcal{O}(\Lambda_{\rm QCD})$. The RG properties of $\Lambda_{s,o}(r,\mu)$ fix the renormalon singularity, up to a normalization constant [18]. If US contributions are neglected,

$$\Lambda_{s,o}(r,\mu) = \text{constant} = N_{s,o}\Lambda_{\rm QCD}$$

$$\Lambda_{\rm QCD} = \nu\, e^{-\frac{2\pi}{\beta_0}\frac{1}{\alpha_{\rm s}(\nu)} - b\ln\alpha_{\rm s}(\nu) + b_0\alpha_{\rm s}(\nu) + \frac{1}{2}b_1\alpha_{\rm s}(\nu)^2 + \ldots}$$

$b, b_1, b_2, \ldots$ are related to the coefficients of the beta function. This structure matches the ambiguity in the definition of the following Borel integral

$$I_{s,o} = \nu\frac{4\pi}{\beta_0}\int_0^\infty du\, e^{-\frac{4\pi}{\beta_0}\frac{u}{\alpha_{\rm s}(\nu)}}\left\{\frac{R_{s,o}}{(1-2u)^{1+b}}\left[1 + c_1(1-2u)\right.\right.$$

$$\left.\left. + c_2(1-2u)^2 + c_3(1-2u)^3 + \ldots\right] + \quad \text{analytical} \quad \text{terms}\right\},$$

By taking $\nu = 1/r$ and expanding about $u = 0$ this expression matches the perturbative series for the potentials $V_{s,o}(r,\mu = 1/r)$. The c_i are given in terms of the coefficients of the β-function. $R_{s,o}$

may be obtained by expanding about $u = 0$

$$R_{s,o} = V^{BT}_{s,o}(u)(1-2u)^{1+b}|_{u=\frac{1}{2}}$$

where $V^{BT}_{s,o}(u)$ are the Borel transform of the series of $V_{s,o}(r,\mu = 1/r)$.

The *RS*-scheme is defined by subtracting the terms in the potentials which emanate from the renormalon singularity at some fix value of ν at each order in PT [19]. These are indeed constant contributions which can be reshuffled in a residual mass term. This scheme greatly improves the convergence of the potential, as shown in fig. 3.

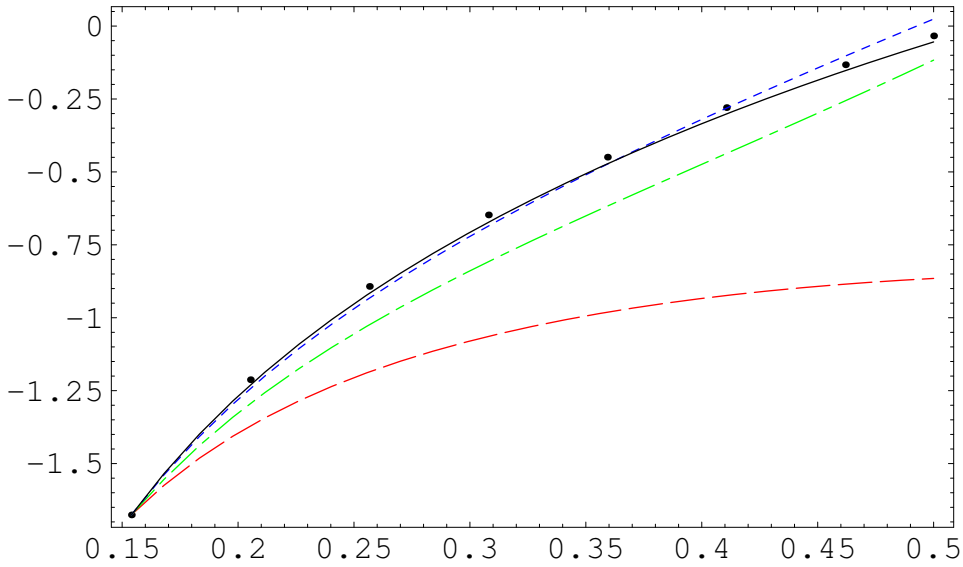

Figure 3: Plot of $r_0(V_{\rm RS}(r) - V_{\rm RS}(r') + E_{latt.}(r'))$ (y-axis) versus r/r_0 (x-axis) at tree (dashed line), one-loop (dash-dotted line), two-loops (dotted line) and three loops (estimate) plus the RG expression for the ultrasoft logs (solid line) compared with the lattice simulations $E_{latt.}(r)$. We set $\nu = \mu = 2.5\, r_0^{-1}$ and $r' = 0.15\, r_0$ ($r_0^{-1} \simeq 400 MeV.$). Plot taken from ref. [17].

However, the analysis above only holds up to two loops. Beyond two loops $\Lambda_{s,o}(r,\mu)$ develope non-trivial anomalous dimensions due to US effects [16],

$$\mu \frac{d}{d\mu}\Lambda_s = -2\frac{\alpha_s C_F}{\pi} V_A^2 r^2 \left[(V_o - V_s)\,(1/r)\right]^2 (\Lambda_o - \Lambda_s)$$
$$\mu \frac{d}{d\mu}\Lambda_o = \frac{2}{N_c^2 - 1}\frac{\alpha_s C_F}{\pi} V_A^2 r^2 \left[(V_o - V_s)\,(1/r)\right]^2 (\Lambda_o - \Lambda_s)$$

These equations can be solved leading to

$$\Lambda_s(r,\mu) = N_s \Lambda_{\rm QCD} + 2C_F(N_o - N_s)\Lambda_{\rm QCD}\, r^2 \left[(V_o - V_s)\,(r)\right]^2 \left(\frac{2}{\beta_0}\ln \alpha_s(\mu)\right)$$
$$\Lambda_o(r,\mu) = N_o \Lambda_{\rm QCD} - \frac{1}{N_c}(N_o - N_s)\Lambda_{\rm QCD}\, r^2 \left[(V_o - V_s)\,(r)\right]^2 \left(\frac{2}{\beta_0}\ln \alpha_s(\mu)\right)$$

The renormalon singularity then becomes

$$I_{s,o} = \nu \frac{4\pi}{\beta_0} \int_0^\infty du\, e^{-\frac{4\pi}{\beta_0}\frac{u}{\alpha_{\rm s}(\nu)}} \left\{ \frac{R_{s,o}}{(1-2u)^{1+b}} [1 + c_1(1-2u) \right.$$
$$+ c_{2;s,o}(1-2u)^2 + c_{3;s,o}(1-2u)^3 + \ldots + d_{1;s,o}(1-2u)^2 \ln(1-2u)$$
$$\left. + \cdots] + \quad \text{analytical} \quad \text{terms} \right\},$$

where c_2, c_3, ... are now different for singlet and octet, and depend on the US anomalous dimensions. Note also that d_1 introduces a new singularity with a logatithmic term.

6. NNNLL calculation

The excellent agreement with lattice data observed in fig. 3 seems to imply that going beyond NNLL is totally unnecessary. However, a calculation exists in the literature which suggest that the NNNLL anomalous dimension for the singlet potential is very large [20], which makes the NNNLL calculation worth addressing. After a closer look at the problem, it turns out that the results provided in [20, 14] are essentially all one needs, from a computational point of view, to put forward the NNNLL expression, as we shall see in the following.

First of all, by analysing the structure of higher orders in the multipole expansion in pNRQCD, one can see that no contribution to the next order of the singlet anomalous dimension arises from that source. Hence, it can be read off the results from [14],

$$\gamma_s(\alpha_{\rm s}) = -\frac{2}{3}\frac{\alpha_{\rm s} C_F}{\pi}\left(1 + 6\frac{\alpha_{\rm s}}{\pi}B\right), \quad B = \frac{-5N_f + C_A(6\pi^2+47)}{108}$$

The octet anomalous dimension requires in principle an independent two loop calculation if attempted in a covariant gauge, as the one used in [20]. However, carrying out this calculation is not necessary. Indeed, both the single and octet anomalous dimensions in pNRQCD are gauge invariant quantities. If one chooses the $A_0 = 0$ gauge, the diagrams which enter the caculation of the octet anomalous dimension are exactly the same as the ones which enter the calculation of the singlet one, and hence both anomalous dimensions are related by trivial color factors,

$$\gamma_o(\alpha_{\rm s}) = -\gamma_s(\alpha_{\rm s})/(N_c^2 - 1)$$

We also need the anomalous dimensions $\gamma_A(\alpha_{\rm s})$ and $\gamma_B(\alpha_{\rm s})$, and the finite pieces of V_A and V_B, at next order. However, we can prove them zero with the following argument. The anomalous dimensions are related to single IR logarithms which arise in the matching calculation, and, of course, the finite pieces of V_A and V_B are also obtained in such a calculation. If we attempt this calculation in the Coulomb gauge, we immediatly see that there is no $\mathcal{O}(\alpha_{\rm s})$ contribution, and hence the finite pieces of V_A and V_B are zero at the required order. Concerning the IR divergences at $\mathcal{O}(\alpha_{\rm s}^2)$, they can only arise fron the diagram in fig. 4. However, this diagram only has a linear IR divergence, and hence induces no contribution to the anomalous dimensions.

As a consequence of the above, the RG equations keep the same structure as at NNLL and can be solved,

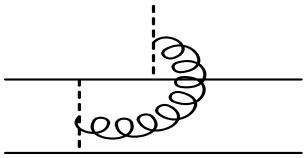

Figure 4:

$$V_s(r,\mu) = V_s(r,1/r) + 2\frac{N_c^2-1}{N_c^2}\left[(V_o-V_s)(r)\right]^3 r^2 \frac{\gamma_{os}^{(0)}}{\beta_0}\left\{\ln\frac{\alpha_s(\mu)}{\alpha_s(1/r)} + \left(-\frac{\beta_1}{4\beta_0}+\frac{\gamma_{os}^{(1)}}{\gamma_{os}^{(0)}}\right)\left[\frac{\alpha_s(\mu)}{\pi}-\frac{\alpha_s(1/r)}{\pi}\right]\right\}$$

$$V_o(r,\mu) = V_o(r,1/r) - \frac{2}{N_c^2}\left[(V_o-V_s)(r)\right]^3 r^2 \frac{\gamma_{os}^{(0)}}{\beta_0}\left\{\ln\frac{\alpha_s(\mu)}{\alpha_s(1/r)} + \left(-\frac{\beta_1}{4\beta_0}+\frac{\gamma_{os}^{(1)}}{\gamma_{os}^{(0)}}\right)\left[\frac{\alpha_s(\mu)}{\pi}-\frac{\alpha_s(1/r)}{\pi}\right]\right\}$$

$$\gamma_{os}^{(0)} = N_c/3, \quad \gamma_{os}^{(1)} = 2N_cB$$

$$\begin{aligned}\Lambda_s(r,\mu) &= N_s\Lambda_{\rm QCD} + 2C_F(N_o-N_s)\Lambda_{\rm QCD}\, r^2\left[(V_o-V_s)(r)\right]^2\left(\frac{2}{\beta_0}\ln\alpha_s(\mu)+\eta_0\alpha_s(\mu)\right)\\ \Lambda_o(r,\mu) &= N_o\Lambda_{\rm QCD} - \frac{1}{N_c}(N_o-N_s)\Lambda_{\rm QCD}\, r^2\left[(V_o-V_s)(r)\right]^2\left(\frac{2}{\beta_0}\ln\alpha_s(\mu)+\eta_0\alpha_s(\mu)\right)\end{aligned}$$

$\eta_0 = \frac{1}{\pi}\left(-\frac{\beta_1}{2\beta_0^2}+\frac{12B}{\beta_0}\right)$

In order to give a consistent formula for $E(r)$ we still need to specify how to count $\Lambda_{\rm QCD}$ with respect to α_s/r. We choose,

$$\frac{1}{r} \gg \frac{\alpha_s}{r} \gg \Lambda_{\rm QCD} \quad \sim \quad \frac{\alpha_s^2}{r}$$

Then at LO we have,

$$E(r) = V_s^{LO}(r).$$

At NLO,

$$E(r) = V_s^{NLO,RS}(r;\nu) + N_s\Lambda_{\rm QCD}$$

where $N_s\Lambda_{\rm QCD}$ is an arbitrary constant. At NNLL we have,

$$E(r) = V_s^{NNLL}(r,\mu) + N_s\Lambda_{\rm QCD}$$

$V_s^{NNLL}(r,\mu)$ is the RG result with initial condition $V_s^{NNLO,RS}(r;\nu)$, $\mu \sim C_A\alpha_s(1/r)/2r$. Finally at NNNLL we have

$$E(r) = V_s^{NNNLL}(r,\mu) + US^{LO}[\mu] + \Lambda_s^{NNLL}(r,\mu)$$

where $N_{s,o}\Lambda_{\rm QCD}$ are arbitrary constants. $US^{LO}[\mu]$ stands for the ultrasoft contribution arising from the leftmost diagram in fig. 1 and $V_s^{NNLL}(r,\mu)$ is the RG result with initial condition $V_s^{NNNLO,RS}(r;\nu)$. Note that two arbitrary constants are necessary at this order in order to account properly for non-perturbative contributions which compete with the weak coupling calculations. This freedom is crucial for the consistency with lattice data displayed in fig. 5

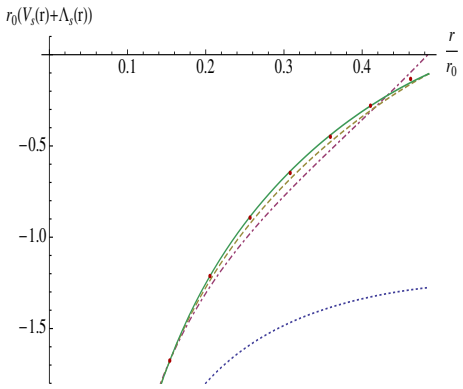

Figure 5: Plot of $r_o(V_s+\Lambda_s)$ as a function of r/r_0 and the lattice data (red points). The dotted blue curve is tree level, the dot-dashed magenta curve is one-loop, the dashed brown curve is two-loops plus leading ultrasoft logarithm resummation and the solid green curve is three-loops (Padé estimate) plus next-to-leading ultrasoft logarithm resummation.

7. Applications

For the NNNLL results above to hold, $\alpha_s/r \gg \Lambda_{\rm QCD}$ is required. For charmonium, bottomonium and B_c the US scale ($\sim \alpha_s/r$) is too low and these results are not expected to be useful beyond NNLL. Note, however, that the NNLL result holds even in the case $\alpha_s/r \sim \Lambda_{\rm QCD}$, since only the UV behavior of the US contributions is required, and hence it is expected to be useful for the ground states of those systems.

The NNNLL result provides a key ingredient for a precision calculation of the t-$\bar{t}$ production cross section at the ILC. This process will allow for a very accurate extraction of the top quark mass, a crucial parameter for standard model calculations. The NNLO result for this process has been available for some time [21]. The proper treatment of the renormalon was crucial to get a stable position for the would-be $1S$ pole. Partial results of NNLL show that the shape of the cross-section becomes much more stable after the log resummations [22]. Partial results at NNNLO also exists [23], and eventually a renormalon and RG analysis of these results may become necessary, for which the NNNLL result above already provides a non-trivial ingredient.

8. Conclusions

The QCD static energy is now essentially known at NNNLL accuracy [16], the only missing ingredient being the $N_f = 0$ piece of the three loop singlet potential, which is in progress [11]. Reaching this level of precision, which includes renormalization group and renormalon analysis, would be unthinkable without a heavy use of effective field theory techniques in pNRQCD. The agreement with lattice data is excellent, and such a level of precision may eventually be relevant for an accurate extraction of the top quark mass at the ILC.

Acknowledgments

I thank Nora Brambilla, Xavier Garcia i Tormo, Antonio Pineda and Antonio Vairo for collaboration on several works related to this talk. I acknowledge financial support from the RTN Flavianet

MRTN-CT-2006-035482 (EU), the FPA2007-60275/ and FPA2007-66665-C02-01/ MEC grants (Spain), and the 2005SGR00564 CIRIT grant (Catalonia).

References

[1] K. G. Wilson, Phys. Rev. D **10**, 2445 (1974).

[2] S. Necco and R. Sommer, Nucl. Phys. B **622**, 328 (2002).

[3] Y. Nambu, Phys. Lett. B **80**, 372 (1979); M. Luscher, K. Symanzik and P. Weisz, Nucl. Phys. B **173**, 365 (1980); M. Luscher and P. Weisz, JHEP **0207**, 049 (2002).

[4] T. Appelquist, M. Dine and I. J. Muzinich, Phys. Rev. D **17**, 2074 (1978).

[5] A. Pineda and J. Soto, Nucl. Phys. Proc. Suppl. **64**, 428 (1998).

[6] N. Brambilla, A. Pineda, J. Soto and A. Vairo, Nucl. Phys. B **566**, 275 (2000).

[7] N. Brambilla, A. Pineda, J. Soto and A. Vairo, Rev. Mod. Phys. **77**, 1423 (2005).

[8] W. Fischler, Nucl. Phys. B **129**, 157 (1977); A. Billoire, Phys. Lett. B **92**, 343 (1980).

[9] M. Peter, Phys. Rev. Lett. **78**, 602 (1997); Nucl. Phys. B **501**, 471 (1997); Y. Schroder, Phys. Lett. B **447**, 321 (1999); B. A. Kniehl, A. A. Penin, M. Steinhauser and V. A. Smirnov, Phys. Rev. D **65**, 091503 (2002).

[10] N. Brambilla, A. Pineda, J. Soto and A. Vairo, Phys. Rev. D **60**, 091502 (1999).

[11] A. V. Smirnov, V. A. Smirnov and M. Steinhauser, Phys. Lett. B **668**, 293 (2008).

[12] F. A. Chishtie and V. Elias, Phys. Lett. B **521**, 434 (2001).

[13] A. Pineda and J. Soto, Phys. Lett. B **495**, 323 (2000).

[14] N. Brambilla, X. Garcia i Tormo, J. Soto and A. Vairo, Phys. Lett. B **647**, 185 (2007).

[15] B. A. Kniehl, A. A. Penin, Y. Schroder, V. A. Smirnov and M. Steinhauser, Phys. Lett. B **607**, 96 (2005).

[16] N. Brambilla, X. Garcia i Tormo, J. Soto and A. Vairo, ANL-HEP-PR-08-57, IFUM-930-FT, UB-ECM-PF 08/03 preprint.

[17] A. Pineda, J. Phys. G **29**, 371 (2003).

[18] M. Beneke, Phys. Lett. B **344**, 341 (1995).

[19] A. Pineda, JHEP **0106**, 022 (2001).

[20] M. Eidemuller and M. Jamin, Phys. Lett. B **416**, 415 (1998).

[21] A. H. Hoang *et al.*, Eur. Phys. J. direct C **2**, 1 (2000).

[22] A. H. Hoang and I. W. Stewart, Phys. Rev. D **67**, 114020 (2003); A. Pineda and A. Signer, Nucl. Phys. B **762**, 67 (2007).

[23] M. Beneke and Y. Kiyo, Phys. Lett. B **668**, 143 (2008); M. Beneke, Y. Kiyo and A. A. Penin, Phys. Lett. B **653**, 53 (2007); M. Beneke, Y. Kiyo and K. Schuller, Phys. Lett. B **658**, 222 (2008); Nucl. Phys. B **714**, 67 (2005).